INTERNATIONAL JOURNAL OF CONTROL, 2016
VOL. 89, NO. 4, 783–792
http://dx.doi.org/10.1080/00207179.2015.1099166

Taylor & Francis
Taylor & Francis Group

Stability domains of the delay and PID coefficients for general time-delay systems

Elham Almodaresi[a], Mohammad Bozorg[a] and Hamid D. Taghirad[b]

[a]Department of Mechanical Engineering, Yazd University, Yazd, Iran; [b]Department of Systems and Control, K.N.Toosi University of Technology, Tehran, Iran

ABSTRACT

Time delays are encountered in many physical systems, and they usually threaten the stability and performance of closed-loop systems. The problem of determining all stabilising proportional-integral-derivative (PID) controllers for systems with perturbed delays is less investigated in the literature. In this study, the Rekasius substitution is employed to transform the system parameters to a new space. Then, the singular frequency (SF) method is revised for the Rekasius transformed system. A novel technique is presented to compute the ranges of time delay for which stable PID controller exists. This stability range cannot be readily computed from the previous methods. Finally, it is shown that similar to the original SF method, finite numbers of singular frequencies are sufficient to compute the stable regions in the space of time delay and controller coefficients.

ARTICLE HISTORY
Received 30 November 2014
Accepted 19 September 2015

KEYWORDS
PID controller; Rekasius substitution; singular frequency method; stability boundaries; uncertain delay

1. Introduction

Time delays are either intrinsic parts of the system dynamics or introduced to the system due to the delays in measurement or actuation. They usually lead to instability and poor performance and difficulties in tuning of the controller coefficients. Different tools are developed to compute the stability margins of time delays. Among them are the linear matrix inequality (LMI) methods (Chen, Gu, & Nett, 1994; Gu, Kharitonov, & Chen, 2003; Nguyen, Ishihara, Krishnakumar, & Bakhtiari-Nejad, 2009) and the frequency-based methods (Almodaresi & Bozorg, 2009; Gu, Niculescu, & Chen, 2005; Sipahi & Olgac, 2005). The LMI methods compute conservative margins for delays, while the frequency-based approaches are less flexible for more complicated cases of multiple input multiple output systems with uncertain models and external disturbances. For controller design, iterative algorithms are suggested to produce some delay-dependent LMIs in Du, Lam, and Shu (2010). Different frequency-based approaches are also taken to define the set of all stabilising PID controllers for processes with fixed time delays, namely the D-decomposition method (Saadaoui, Elmadssia, & Benrejeb, 2008) and the parameter space method (Hohenbichler & Ackermann, 2003), which both graphically present the set of all stabilising PID controllers for processes with fixed time delays. The singular frequency (SF) method (Bajcinca, 2001, 2006; Hohenbichler, 2009) formulates the stability boundary crossings, as a matrix rank deficiency problem. Another widely applied approach to design PID controllers for time-delay systems is the extension of the Hermit–Biehler theorem for quasi-polynomials (Ou, Zhang, & Yu, 2009). This theorem proves the interlacing property of roots of the real and imaginary parts of a stable polynomial. A couple of works have also employed the Nyquist plot properties to compute the delay stability margins for the second-order and all-pole delay systems (Lee, Wang, & Xiang, 2010; Xiang, Wang, Lu, Nguyen, & Lee, 2007). The Lambert W function is used in Yi, Nelson, and Ulsoy (2007) to compute an analytical solution for delay differential equations. However, numerical computations are required in some stages of the algorithm. A certain value is assigned to the time delay. The PI controller is computed for first-ordered delay systems by Yi, Nelson, and Ulsoy (2013) combining the latter method with the pole-placement technique. An eigenvalue-based method is also employed by Michiels and VyhlíDal (2005) and Michiels, Vyhlídal, and Zítek (2010) to stabilise delay equations with certain time delays. However, the effect of the small delay perturbations is investigated on the stability. An uncertainty delay range is considered by Emami and Watkins (2009) to present a graphical method for computing all robust stabilising controllers. Again, the delay is assumed a fixed value, the mean of the uncertainty range. Also, the controller coefficients and a robust performance parameter are swept in this method.

In practice, for many time-delayed systems, delays are uncertain but bounded in defined ranges. For such systems, assuming fixed delays leads to design of fragile

CONTACT Mohammad Bozorg bozorg@yazd.ac.ir

controllers. This is illustrated in Almodaresi and Bozorg (2015) by showing the high sensitivity of the stability of time-delay systems to small values of delay perturbation. Few methods are so far presented to determine the stable regions in the space of the uncertain delay and the controller coefficients. Among them are the works of Almodaresi and Bozorg (2014, 2015) which deal with the special cases of first- and second-order delay systems. The phase conditions of the open loop transfer functions are employed in Almodaresi and Bozorg (2014) to compute the maximum allowable delay for which some stable gain exists. Also, Nyquist plot properties are used in Almodaresi and Bozorg (2015) to compute the regions in the plane of the uncertain delay and the PI controller coefficients, inside which stable gain intervals exist. Both approaches are applicable just for the first- and the second-order plants containing delays. However, the uncertain delay and controller coefficients are not required to be swept to plot the stability boundaries in Almodaresi and Bozorg (2015).

Time delay is considered a fixed value in previous works when computing the stabilising range of PID controller coefficients. In this paper, we aim to consider the delay as an uncertain parameter and compute the stable domain in the space of $k_I - k_D - \tau$, while calculating the maximum allowable delay for which a stable PID controller exists. In the next section, the fundamental results of the SF method are presented (Bajcinca, 2001). This method is employed by Hohenbichler (2009) to compute the stable regions in the space of PID coefficients, for systems with fixed delays. An inequality constraint is used in Hohenbichler (2009) as a stability condition to compute the allowable k_p-intervals. However, if delay is assumed uncertain, both sides of the inequality will be nonlinearly dependent on the time delay. This introduces complexities to this problem and requires additional numerical computations and tackling of convergence problems.

The most important contribution of this paper is to present an analytic technique for computing the exact delay range in which a stabilising PID controller exists. This technique is based on transforming the system equations by the Rekasius substitution to a new set of equations that can be handled more conveniently. To achieve this, the SF method is modified and new results are obtained for the transformed system. After computing the stabilisable delay range, the SF method is used to plot the stability range in the plane of K_I–K_D, by sweeping the delay in the computed range. It is also shown that the singular frequencies of the Rekasius transformed system (RTS), which are computed from two generator functions, do not interlace before a certain frequency. It is also proved that the intersections of the singular lines with the k_I-axis, follow a special trend, which can be used to compute the stability boundaries.

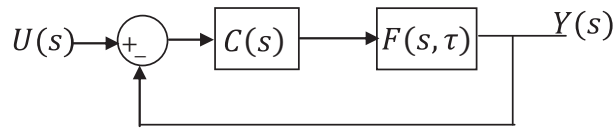

Figure 1. Block diagram of a time-delay system.

The rest of the paper is organised as follows. In Section 2, the existing SF results for the time-delay systems with fixed delays are explained. Section 3 introduces the uncertainty in the time delay and extends the results of Section 2 to this case. The problem of drawing the stability boundaries in the space of the PID controller coefficients and the uncertain delay is addressed in this section. First, the framework of the SF method is revised for the RTS. Then, a technique is presented to compute the delay stability interval. Singular frequencies, singular lines and crossing direction concepts are computed for the RTS. A practical case study is presented in Section 4 to demonstrate the implementation of the proposed method.

2. A singular frequency method

Consider the block diagram of a time-delay plant

$$F\ (s,\tau) = N(s)\, e^{-\tau s}/R(s)\ , \tag{1}$$

in which $N(s)$ and $R(s)$ are polynomials of degrees m and r, respectively, where $m < r$. Also, $C\ (s) = k_I/s\ + k_p + k_D s$ is a PID controller as in Figure 1, where k_I, k_p and k_D are the controller coefficients. The characteristic equation is

$$P\ (s,\tau) = D(s) + \left(k_I + k_p s + k_D s^2\right) N(s)\, e^{-\tau s}, \tag{2}$$

where $D\ (s) = sR(s)$.

Assume $N\ (s) = a_0\ + \cdots + a_m s^m$, $a_m \neq 0$ and $D\ (s) = b_0\ + \cdots + b_{n-1}s^{n-1} + s^n$. Obviously, $b_0 = 0$. This system is retarded, if $q > 2$ and is neutral, if $q = 2$. The characteristic equation (2) has an infinite number of roots due to the exponential delay term. All of these roots must be located in the left half-plane (LHP) to ensure the stability. The controller coefficients where the roots of Equation (2) cross the stability boundary are the *root crossing boundaries*. To compute the crossing boundaries, where the roots of Equation (2) cross the imaginary axis, $s = j\omega$ is substituted in Equation (2). Then, by decomposing the characteristic equation into the real and imaginary parts, two equations are obtained (Hohenbichler, 2009),

$$k_I - k_D\,\omega^2 = y_1(\omega)\cos(\tau\omega) - y_2(\omega)\sin(\tau\omega), \tag{3-a}$$

$$k_p = \left[y_1(\omega)\sin(\tau\omega) + y_2(\omega)\cos(\tau\omega)\right]/\omega = y(\omega), \tag{3-b}$$

in which,

$$\begin{aligned} y_1(\omega) &= \left(N_r(\omega)D_r(\omega) \right. \\ &\quad \left. + N_i(\omega)D_i(\omega)\right)/\left(N_r(\omega)^2 + N_i(\omega)^2\right) \\ y_2(\omega) &= \left(N_i(\omega)D_r(\omega) \right. \\ &\quad \left. - N_r(\omega)D_i(\omega)\right)/\left(N_r(\omega)^2 + N_i(\omega)^2\right), \end{aligned} \tag{4}$$

where $N_r(\omega)$, $N_i(\omega)$, $D_r(\omega)$ and $D_i(\omega)$ are the real and imaginary parts of $N(j\omega)$ and $D(j\omega)$, respectively. Equation (3-a) is independent of k_p and Equation (3-b) is independent of k_I and k_D. For a defined value of τ and k_p, Hohenbichler (2009) computes the singular frequencies $\omega_1, \omega_2, \ldots$ by solving $y(\omega) = k_p$ from Equation (3-b). $y(\omega)$ is called the generator function and it is shown that the sign of the derivative of this function change alternately at the singular frequencies, i.e.

$$\begin{aligned} &\operatorname{sgn}\left[\frac{\partial y(\omega)}{\partial\omega}|_{\omega_i}\right] \neq \operatorname{sgn}\left[\frac{\partial y(\omega)}{\partial\omega}|_{\omega_{i+1}}\right],\ i = 1, 2, \ldots \\ &\operatorname{sgn}\left[\frac{\partial y(\omega)}{\partial\omega}|_{\omega_i}\right] = \operatorname{sgn}\left[\frac{\partial y(\omega)}{\partial\omega}|_{\omega_{i+2}}\right],\ i = 1, 2, \ldots \end{aligned} \tag{5}$$

The singular lines, which form the root crossing boundaries, are then obtained in the $k_I - k_D$ plane, by substituting the computed singular frequencies in Equation (3-a). It is also shown that, although an infinite number of singular frequencies is computed from Equation (3-b), a finite number of the frequencies need to be considered to compute the singular lines that form the stability crossing boundaries. This claim is proved by showing that from a certain frequency onward, singular frequencies interlace with an interval of π/τ. Let us call this frequency, the *periodicity frequency*.

To account for the changes in the number of unstable roots of the characteristic equation on the two sides of a singular line, the concept of root crossing direction is introduced. This sign change or the crossing direction is investigated in Bajcinca (2001, 2006) and Hohenbichler (2009).

3. Uncertain time delay

In this section, the SF method is extended for the case of systems with uncertain delays. The main problem caused by assuming delay uncertainty in Equation (3) is that the singular frequencies and the periodicity frequency will depend nonlinearly on the value of the delay, resulting in a set of nonlinear equations. To compute the stable regions in the space of $k_I - k_D - \tau$, first one needs to compute the stable range of delay and to evaluate the relation between the delay and the periodicity frequency. In this paper, the Rekasius substitution is employed as an assistant tool to evaluate these. First, the characteristic equation is put into a matrix form using the Rekasius substitution. Unlike the SF method, in which one generator function (3-b) is computed, here two generator functions are derived to compute the singular frequencies for the RTS. The computed singular frequencies are obtained as functions of the delay. It is shown that the singular frequencies of the two functions do not necessarily interlace. However, we will prove that they interlace from a certain frequency (periodicity frequency) onward. Based on this result, a method is presented to compute the maximum delay for which stable PID controllers exist. Then, by computing two sets of singular lines from singular frequencies, the features of the resulting singular lines are investigated. The singular lines are evaluated in the $k_D - k_I$ plane and the root crossing direction is computed for each singular line. By sweeping τ in the stable delay interval, stable regions in the $k_I - k_D - \tau$ space are calculated.

3.1 Singular frequency method for RTS

If the exponential delay term in Equation (2) is substituted by a bilinear rational function of a new parameter T (Rekasius, 1980),

$$e^{-\tau s} = (1 - Ts)/(1 + Ts),\ s = j\omega, \tag{6}$$

in which,

$$\tau = \frac{2}{\omega}\left[\tan^{-1}(T\omega) + k\pi\right],\ k = 1, 2, \ldots, \tag{7}$$

the characteristic equation of the RTS is obtained as

$$\begin{aligned} P'(s, T) &= D(s)(1 + Ts) \\ &\quad + \left(k_I + k_p s + k_D s^2\right)N(s)(1 - Ts). \end{aligned} \tag{8}$$

When Equation (7) holds, the roots of Equations (8) and (2) are identical. Define $P'(j\omega, T) = H(\omega, T) + jG(\omega, T)$. Putting $P(j\omega, T) = 0$ in a matrix equation form leads to

$$\begin{aligned} \begin{bmatrix} H(\omega, T) \\ G(\omega, T) \end{bmatrix} &= A(\omega, T)\left\{\begin{bmatrix} 1 & -\omega^2 \\ 0 & 0 \end{bmatrix}\begin{bmatrix} k_I \\ k_D \end{bmatrix} + \begin{bmatrix} 0 \\ \omega k_p \end{bmatrix}\right\} \\ &\quad + B(\omega, T) = 0, \end{aligned} \tag{9}$$

where

$$A\ (\omega, T) = \begin{bmatrix} N_r(\omega) + T\omega N_i & T\omega N_r(\omega) - N_i(\omega) \\ N_i(\omega) - T\omega N_r(\omega) & N_r(\omega) + T\omega N_i(\omega) \end{bmatrix}, \tag{10}$$

$$B\ (\omega, T) = \begin{bmatrix} D_r(\omega) - T\omega D_i(\omega) \\ D_i(\omega) + T\omega D_r(\omega) \end{bmatrix}. \tag{11}$$

Since $A(\omega, T)$ is a nonsingular matrix, define $h(\omega, T)$ and $g(\omega, T)$ as

$$\begin{bmatrix} h(\omega, T) \\ g(\omega, T) \end{bmatrix} = A(\omega, T)^{-1} \begin{bmatrix} H(\omega, T) \\ G(\omega, T) \end{bmatrix}. \tag{12}$$

Then,

$$h\ (\omega, T) = k_I - k_D\omega^2 + p_1\ (\omega, T) = 0, \tag{13}$$

$$g\ (\omega, T) = k_p\omega + p_2\ (\omega, T) = 0, \tag{14}$$

$$p_1\ (\omega, T) = \frac{\left[A_r(\omega)\left(1 - T^2\omega^2\right) + 2A_i(\omega)\, T\omega\right]}{\left[\Delta_N(\omega)\left(1 + T^2\omega^2\right)\right]}, \tag{15}$$

$$p_2\ (\omega, T) = \frac{\left[-A_i(\omega)\left(1 - T^2\omega^2\right) + 2A_r(\omega)\, T\omega\right]}{\left[\Delta_N(\omega)\left(1 + T^2\omega^2\right)\right]}, \tag{16}$$

$$A_r\ (\omega) = N_r\ (\omega)\, D_r(\omega) + N_i(\omega)\, D_i(\omega), \tag{17}$$

$$A_i\ (\omega) = N_i\ (\omega)\, D_r(\omega) - N_r(\omega)\, D_i(\omega), \tag{18}$$

$$\Delta_N\ (\omega) = N_r^2\ (\omega) + N_i^2(\omega). \tag{19}$$

Equations (13) and (14) are functions of ω and T, while Equation (3) is a function of ω and τ. The parameters set, where $h(\omega, T) = g(\omega, T) = 0$, is the same set for which $P(j\omega, T) = 0$. For a fixed k_p, the frequencies that satisfy Equation (14) define the singular frequencies. By substituting these frequencies into Equation (13), singular lines (stability crossing boundaries) are derived.

3.2 Singular frequencies of generator functions

In this subsection, it is shown that the singular frequencies of the RTS system in Equation (9) are obtained from two generator functions, while these frequencies are computed from the generator function (3-b) in the SF method. Solving Equation (14) for T, two solutions are computed:

$$T_1\ (\omega) = \left[-A_r(\omega) + \sqrt{u_1(\omega)}\right] / \omega.u_2(\omega), \tag{20}$$

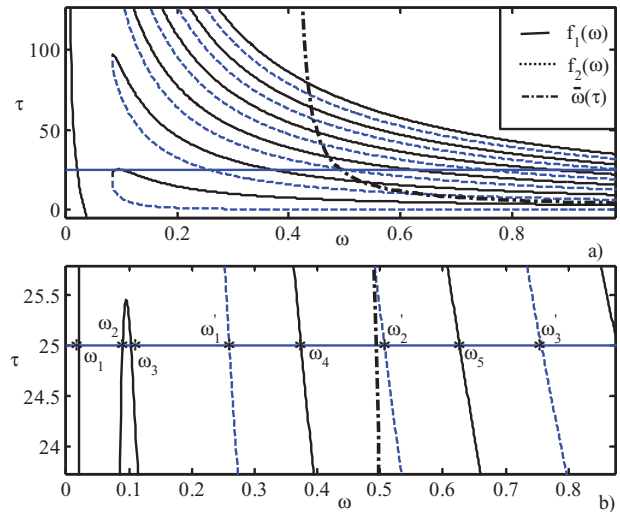

Figure 2. (a) The diagrams $f_1(\omega)$ and $f_2(\omega)$ for $k = 0, , 5$. (b) Frequency roots of $f_1\ (\omega) = 25$ and $f_2(\omega) = 25$. The curve $\bar{\omega}(\tau)$ is introduced in the subsection 'stable delay interval'.

$$T_2\ (\omega) = \left[-A_r(\omega) - \sqrt{u_1(\omega)}\right] / \omega.u_2(\omega) \tag{21}$$

where

$$u_1\ (\omega) = \Delta_N\ (\omega)\left(\Delta_D(\omega) - k_p^2\omega^2\Delta_N(\omega)\right), \tag{22}$$

$$u_2\ (\omega) = k_p\,\omega\Delta_N(\omega) + A_i(\omega), \tag{23}$$

in which $\Delta_D(\omega) = |D(j\omega)|^2$ and $A_r(\omega), A_i(\omega)$ and $\Delta_N(\omega)$ are defined, respectively, in Equations (18) and (19). Substituting $T_1(\omega)$ and $T_2(\omega)$ for T in Equation (7),

$$\tau = f_1\ (\omega) = \frac{2}{\omega}\left[\tan^{-1}(\omega.T_1(\omega)) + k\pi\right], \quad k = 1, 2, \ldots, \tag{24}$$

$$\tau = f_2\ (\omega) = \frac{2}{\omega}\left[\tan^{-1}(\omega.T_2(\omega)) + k\pi\right], \quad k = 1, 2, \ldots, \tag{25}$$

are, respectively, computed. By putting the imaginary part of $P(j\omega, T)$ in Equation (8) equal to 0, two generator functions of singular frequencies as $f_1(\omega) = \tau$ and $f_2(\omega) = \tau$ are obtained. By solving them, two sets of frequencies are obtained, respectively, denoted by $\Omega = \{\omega_1, \omega_2 \ldots\}$ and $\Omega' = \{\omega_1', \omega_2', \ldots\}$. Now, it is shown through an example that the singular frequencies $\omega \in \Omega$ and $\omega' \in \Omega'$ do not necessarily interlace. The diagrams $f_1(\omega)$ and $f_2(\omega)$ are plotted in Figure 2(a), for $p(s, \tau)$ in Equation (2) such that

$$N(s) := -0.2679\,(1 - 41.6667s), \quad D(s) := s\left(279.03s^2 - 2.9781s + 1\right). \tag{26}$$

Figure 2(b) shows the singular frequencies for a fixed delay value $\tau = 25s$ as

$$\Omega = \{0.0207,\ 0.0898, 0.1033, 0.374, 0.6266, \ldots\},$$
$$\Omega' = \{0.2598, 0.5069,\ 0.7568, 1.007, 1.2583, \ldots\}. \quad (27)$$

From Figure 2(b), it is obvious that the singular frequencies do not interlace. Furthermore, the sign of the derivative of their generator functions do not interlace, i.e., $\mathrm{sgn}(\partial f_1(\omega)/\partial\omega), \omega \in \Omega$ and $\mathrm{sgn}(\partial f_2(\omega)/\partial\omega), \omega' \in \Omega'$ do not change alternately. This is the counterpart of the interlacing property of the derivative sign of the generator function $y(\omega)$ in the SF method, which was shown in Equation (5). Although the frequencies of the sets Ω and Ω' do not necessarily interlace, they interlace from a certain frequency onward with a periodicity of π/τ. This concept, which is shown via the curve $\bar{\omega}(\tau)$ on Figure 2, will be discussed later.

Definition 1: Define

$$\bar{r} = \begin{cases} (m+n)/2 \text{ if } m+n \text{ even} \\ (m+n-1)/2 \text{ if } m+n \text{ odd} \end{cases}. \quad (28)$$

where m and n are, respectively, the degrees of $N(s)$ and $R(s)$. Also, define the following conditions:

$$\text{C.1}: (a_m > 0 \,\&\, \bar{r} \text{ even}) \text{ or } (a_m < 0 \,\&\, \bar{r} \text{ odd}), \quad (29)$$

$$\text{C.2}: (a_m > 0 \,\&\, \bar{r} \text{ odd}) \text{ or } (a_m < 0 \,\&\, \bar{r} \text{ even}), \quad (30)$$

where a_m is the coefficient of s^m in $N(s)$.

Proposition 1: For a large enough value $l \in \mathbb{N}$, the singular frequencies $\omega_j \in \Omega$ and $\omega'_j \in \Omega'$, $j = l, l+1, \ldots$ interlace with the periodicity of π/τ.

Proof: By substituting Equations (20) and (21), respectively, into Equations (24) and (25), the following equations are obtained:

$$e(\omega) = \cos(\tau\omega/2)\left(\sqrt{u_1(\omega)} - A_r(\omega)\right) - \sin\left(\frac{\tau\omega}{2}\right)u_2(\omega) = 0, \quad (31)$$

$$e'(\omega) = \cos(\tau\omega/2)\left(\sqrt{u_1(\omega)} + A_r(\omega)\right) + \sin(\tau\omega/2)\,u_2(\omega) = 0 \quad (32)$$

The roots of $e(\omega)$ and $e'(\omega)$, respectively, define the SF sets Ω and Ω'. Obviously, these sets depend on the delay value. Denote the roots of the dominant terms of $e(\omega)$ and $e'(\omega)$ by ω^∞ and ω'^∞. It can be easily checked that, for high frequencies, the root chains of $e(\omega)$ and $e'(\omega)$ lie on the roots of $\sin(\tau\omega/2) = 0$ and $\cos(\tau\omega/2) = 0$, respectively, if m and n are even numbers and Condition C.1 in Equation (29) is satisfied, or if m and n are odd numbers and C.2 holds. Hence,

$$\omega^\infty = \frac{2k\pi}{\tau}, \quad \omega'^\infty = \frac{2k\pi}{\tau} + \frac{\pi}{\tau}. \quad (33)$$

For the case that m and n are even numbers and C.2 holds or m and n are odd numbers and C.1 holds, $\omega^\infty = 2k\pi/\tau + \pi/\tau$ and $\omega'^\infty = 2k\pi/\tau$ are obtained. The root chains of $e(\omega)$ and $e'(\omega)$ ultimately lie on the roots of

$$\tan(\tau\omega/2) = -1, \quad (34)$$

$$\tan(\tau\omega/2) = 1, \quad (35)$$

respectively, if m and n are, respectively, even and odd numbers and C.1 holds or if m and n are, respectively, odd and even numbers and C.2 holds. In this case, $\omega^\infty = 2k\pi/\tau - \pi/2\tau$ and $\omega'^\infty = 2k\pi/\tau + \pi/2\tau$ hold. For the case that m and n are, respectively, even and odd numbers and C.2 holds or m and n are, respectively, odd and even numbers and C.1 holds, $\omega^\infty = k\pi/\tau + \pi/2\tau$ and $\omega'^\infty = 2k\pi/\tau - \pi/2\tau$ are obtained.

For all above cases, $|\omega^\infty - \omega'^\infty| = \pi/\tau$ holds. Therefore, a large enough value $l \in \mathbb{N}$ exists such that

$$\left|\left|\omega_j - \omega'_{j+\bar{j}}\right| - \pi/\tau\right| \le \varepsilon/\tau,\ \varepsilon \ll 1,\ j = l, l+1, \ldots, \quad (36)$$

where $\bar{j}$ is an integer number. Obviously, l depends on the small value ε. Hence, the proposition is proved.

The above proof indicates that the root chains of $e(\omega)$ and $e'(\omega)$ ultimately lie on the roots of two sinusoidal functions with a phase difference of $\pi/2$. Hence, l is a finite number depending on ε.

Remark 1: Note that the indices of ω_j and $\omega'_{j+\bar{j}}$ in Equation (36) are not necessarily identical. For instance, the singular frequencies (27) tend to the periodicity of π/τ with precision $\varepsilon = 0.2$ for the sequence $\omega'_2, \omega_5, \omega'_3, \omega_6, \omega'_4, \ldots$, which are the frequencies $\omega_j \in \Omega$, $\omega'_{j-3} \in \Omega'$ for $j \ge 5$ (Figure 2).

Definition 2: The high singular frequencies are the frequencies $\omega_j \in \Omega$ and $\omega'_{j+\bar{j}} \in \Omega'$, $j = l, l+1, \ldots$, $\bar{j} \in \mathbb{Z}$, such that Equation (36) holds. Also, define the periodicity frequency

$$\bar{\omega} = \max\left\{\omega_l, \omega'_{l+\bar{j}}\right\}, \quad (37)$$

such that the singular frequencies larger than that, interlace with the periodicity of π/τ.

Using the above results, a method is presented in the next subsection to compute the stable delay interval.

3.3 Stable delay intervals

In this subsection, a new method is presented to compute the delay interval for which stabilising PID controllers exist. The SF sets Ω and Ω', computed, respectively, from Equations (24) and (25), change when the delay is changed. From Definition 2, all the singular frequencies greater than $\bar{\omega}$ almost reach the periodicity π/τ. Obviously, $\bar{\omega}$ depends on the delay. Define $z(\tau)$ as the number of singular frequencies in the interval $(0, \bar{\omega}(\tau))$. A necessary condition for the stability of Equation (2) is that (Hohenbichler, 2009)

$$z(\tau) \geq z_{\min}(\tau), \tag{38}$$

$$z_{\min}(\tau) = \operatorname{ceil}\left[\frac{l + 2m_R + m_I + m_o + \operatorname{rem}(m_o, 2) - \hat{m}_I}{2} + \frac{\bar{\omega}(\tau).\tau}{\pi}\right] - 1 \tag{39}$$

in which, m_R and m_o are, respectively, the number of unstable roots and the roots located at the origin, of $N(s)$. m_I is the number of roots $s = j\omega_j$ of $N(s)$ with $\omega_j \neq 0$. $\hat{m}_I$ of the m_I roots of $N(s)$ possess an odd order and ensure an existing limit $\lim_{\omega\to\omega_j} |p(j\omega, \tau)/N(j\omega)|$. $N(s)$ and $p(s, \tau)$ are, respectively, defined in Equations (1) and (2). Also, $\operatorname{rem}(m_o, 2)$ denotes the remainder of the division of m_o by 2.

Equation (39) is a necessary condition for the stability. Hence, it can be used to find a stable k_p sweeping interval when a certain value is assigned to the time delay. However, assuming the delay to be uncertain, both sides of the inequality depend on the delay value. Therefore, $\bar{\omega}(\tau)$ must be evaluated first to compute $z_{\min}(\tau)$. Here, a technique is presented to find $\bar{\omega}(\tau)$.

From Equation (36), there exists a large enough value $l \in \mathbb{N}$, for each known delay τ, such that $|\omega_l - \omega'_{l+\bar{j}}|$ equals to $(\pi + \varepsilon)/\tau$ or $(\pi - \varepsilon)/\tau$, $\varepsilon \ll 1$ (Proposition 1). Define $\omega'_{l'} = \omega'_{l+\bar{j}}$ for simplicity. Without loss of generality, assume

$$\omega_l - \omega'_{l'} = (\pi - \varepsilon)/\tau\,. \tag{40}$$

Since ω_l and $\omega'_{l'}$ are the roots of Equations (24) and (25), respectively, one has

$$\tau = 2\left[\tan^{-1}(\omega_l.T_1(\omega_l)) + k\pi\right]/\omega_l, \tag{41}$$

$$\tau = 2\left[\tan^{-1}\left(\omega'_{l'}.T_2\left(\omega'_{l'}\right)\right) + k\pi\right]/\omega'_{l'}, \tag{42}$$

where k is an integer number. By substituting τ from Equation (40) into Equations (41) and (42)

$$\omega_l T_1(\omega_l) = \left(c_1 + c_2\left(\omega'_{l'}\right)\right)/\left(1 - c_1 c_2\left(\omega'_{l'}\right)\right), \tag{43}$$

is obtained, where $c_1 = \tan((\pi - \varepsilon)/2)$ and $c_2(\omega'_{l'}) = \omega'_l\, T_2(\omega'_{l'})$. By substituting ω_l into Equation (20),

$$\omega_l T_1(\omega_l) = \left(-A_r(\omega_l) + \sqrt{u_1(\omega_l)}\right)/u_2(\omega_l) \tag{44}$$

holds. Define the right-hand side of Equation (43) as $c'(\omega'_{l'})$. Then, Equation(43) simplifies to

$$A_r(\omega_l) + c'\left(\omega'_{l'}\right) u_2(\omega_l) = \sqrt{u_1(\omega_l)}\,, \tag{45}$$

by using Equation (44). For a fixed $\omega'_{l'}$, Equation (45) is a nonlinear function of ω_l. Square two sides of Equation (45) to obtain the linear equation

$$\left[A_r(\omega_l) + c'\left(\omega'_{l'}\right) u_2(\omega_l)\right]^2 = u_1(\omega_l)\,. \tag{46}$$

Then, ω_l is computed from the polynomial function (46) by sweeping $\omega'_{l'}$. Obviously, those pairs of ω_l,$\omega'_{l'}$ are acceptable which satisfy Equation (45). For each pair of ω_l,$\omega'_{l'}$, τ is evaluated from Equation (40). Then, $\bar{\omega}(\tau)$ is computed from Equation (37). Now, $z_{\min}(\tau)$ is calculated by substituting $\bar{\omega}(\tau)$ into Equation (39). Also, $z(\tau)$ is the number of singular frequencies in the interval $(0, \bar{\omega}(\tau))$. Finally, the stable delays are the delays satisfying Equation (38). The $\bar{\omega}(\tau)$ diagram is plotted in Figure 2 for the system of Equation (26). More explanations are provided at the case study section.

3.4 Singular lines and root crossing direction

In this subsection, the singular lines and the root crossing directions are investigated for the RTS (8).

Definition 3: Define two sets of singular lines $L = \{\ell_1, \ell_2, \ldots\}$ and $L' = \{\ell'_1, \ell'_2, \ldots\}$ computed, respectively, by substituting the singular frequencies of the sets Ω and Ω' into Equation (13). Also, define the k_I-intersection, as the intersection of a singular line with the k_I axis, denoted by k_I^*.

Remark 2: The more stable side of a singular line is defined as its side with less closed-loop poles which is indicated as the unmarked side in all graphs of this paper.

Lemma 1: The k_I-intersections of the singular lines $\ell_j \in L$ and $\ell'_j \in L'$, $j = 1, 2, \ldots$ are, respectively, negative and positive.

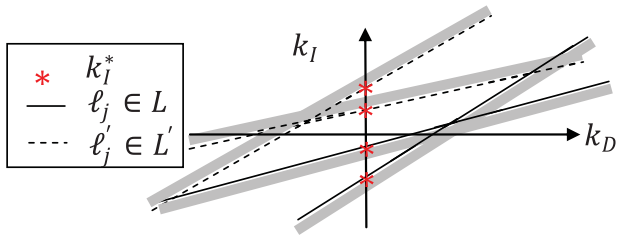

Figure 3. Singular lines and k_I-intersections on the $k_D - k_I$ plane.

Proof: From Equation (15), $p_1(\omega, T)$ is rewritten as

$$p_1(\omega, T) = \frac{\Delta_R(\omega) - k_p^2\omega^2\Delta_N(\omega)}{A_r(\omega) + T\omega A_i(\omega) + T\omega^2 k_p\Delta_N(\omega)}, \tag{47}$$

by using Equations (14) and (16). Also, $k_I^* = -p_1(\omega, T)$ is obtained from Equation (13). Substitute T_1 and T_2, respectively, from Equations (20) and (21), for T in Equation (47). Then,

$$k_I^* = \begin{cases} -f(\omega_j), & \omega_j \in \Omega \\ f(\omega_j'), & \omega_j' \in \Omega' \end{cases}, \quad f(\omega) = \sqrt{\frac{\Delta_D - k_p^2\Delta_N\omega^2}{\Delta_N}}. \tag{48}$$

Assume $f(\omega) \neq 0, \ \forall\omega$. Since $f(\omega)$ is positive for all frequencies, the lemma is proved (Figure 3).

Corollary 1: From Lemma 1, singular lines $\ell_j \in L$ and $\ell_j' \in L'$, $j = 1, 2, \ldots$ are, respectively, computed from

$$\ell_j : \ k_I - k_D\omega_j^2 + f(\omega_j) = 0, \ \omega_j \in \Omega, \tag{49}$$

$$\ell_j' : k_I - k_D\omega_j'^2 - f(\omega_j') = 0, \ \omega_j' \in \Omega'. \tag{50}$$

□

In the rest of this subsection, the root crossing direction is computed for the singular lines (49) and (50). Assume the singular line in Figure 4 is crossed in the direction $\delta k_I > 0$. The direction of crossing of eigenvalues of the system is defined by a root crossing index (Bajcinca, 2006)

$$e_I = \text{sgn}\left[\text{Re}\left(ds/dk_I\right)\right]|_{s=j\omega}. \tag{51}$$

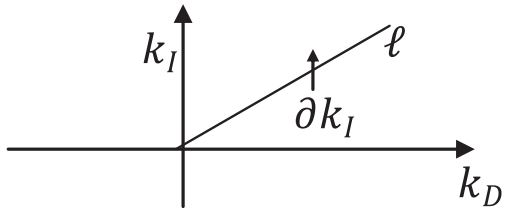

Figure 4. The root crossing direction for a singular line ℓ.

Suppose that the singular line is crossed in the direction $\delta k_I > 0$. The system's eigenvalues cross the imaginary axis towards the right half plane (RHP) if $e_I = 1$ and towards the LHP if $e_I = -1$. The following theorem computes the root crossing direction of the singular lines of the RTS (8).

Theorem 1: The root crossing index for the singular lines (49) and (50) is evaluated from

$$e_I = -\text{sgn}\left(\frac{\partial g(\omega, T)}{\partial\omega} + \frac{\partial g(\omega, T)}{\partial T}\frac{\partial T(\omega)}{\partial\omega}\right). \tag{52}$$

where $g(\omega, T)$ is defined in Equation (14), and $T(\omega) = [\tan(\tau\omega/2)]/\omega$ is computable from Equation (7).

Proof: Since k_D and k_p are fixed, $P(s, T)$ is a function of s, T and k_I from Equation (8). Furthermore, since $P(s, T) = 0$, the total differential equation $dP(s, T)$ is equal to 0 (Bajcinca, 2006). Hence,

$$dP = \frac{\partial P}{\partial s}ds + \frac{\partial P}{\partial T}\frac{\partial T}{\partial s}ds + \frac{\partial P}{\partial k_I}d\,k_I = 0. \tag{53}$$

From Equation (53),

$$\frac{ds}{dk_I} = -\frac{\partial P}{\partial k_I}\Big/\left(\frac{\partial P}{\partial s} + \frac{\partial P}{\partial T}\frac{\partial T}{\partial s}\right), \tag{54}$$

holds. By substituting $P(j\omega, T) = G(\omega, T) + jH(\omega, T)$ and $s = j\omega$ into Equation (54), e_I is computed from Equations (51) and (54) as

$$e_I = \text{sgn}\begin{vmatrix} \frac{\partial G(\omega, T)}{\partial k_I} & \frac{\partial G(\omega, T)}{\partial\omega} + \frac{\partial G(\omega, T)}{\partial T}\frac{\partial T}{\partial\omega} \\ \frac{\partial H(\omega, T)}{\partial k_I} & \frac{\partial H(\omega, T)}{\partial\omega} + \frac{\partial H(\omega, T)}{\partial T}\frac{\partial T}{\partial\omega} \end{vmatrix}. \tag{55}$$

Then, Equation (55) is simplified to

$$e_I = \text{sgn}\left[-|A(\omega, T)|\left(\frac{\partial g(\omega, T)}{\partial\omega} + \frac{\partial g(\omega, T)}{\partial T}\frac{\partial T}{\partial\omega}\right)\right], \tag{56}$$

by using the relationship (12) between $H(\omega, T)$, $G(\omega, T)$ and $h(\omega, T), g(\omega, T)$, where $|.|$ is the determinant function. From Equation (10), $|A(\omega, T)| = \Delta_N(\omega)(1 + T^2\omega^2)$ holds. Since $\Delta_N(\omega)$ in Equation (19) is non-negative for all frequencies, Equation (52) holds.

It is proved in Hohenbichler (2009) that for each certain delay, only the singular lines corresponding to the singular frequencies smaller than the periodicity frequency are needed to be computed. It is also shown that the stable region which is a polygon for retarded systems can be described by the limit of a sequence of polygons for

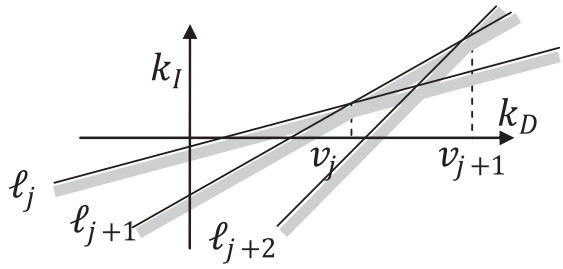

Figure 5. The singular lines and their intersections.

neutral systems. Detailed proof can be found in Hohenbichler (2009). □

Remark 3: It can be shown that the singular lines of the RTS, corresponding to the frequencies higher than the periodicity frequency have some special features. The more stable side of the singular lines ℓ_j, $j = l, l+1, \ldots$ points to the side where k_I increases. On the one hand, all singular lines of the set L intersect with the negative k_I-axis (Lemma 1). Therefore, the more stable side of $\ell_j \in L$, $j = l, l+1, \ldots$ always points to the origin (Figure 5). On the other hand, the k_D junctions of singular lines ℓ_j, $j = l, l+1, \ldots$ move increasingly to the right half-plane for a retarded system (Figure 5) and tend to a positive value for a neutral system (Hohenbichler, 2009). Therefore, the k_D junctions $v_j \in V$ move outward from the stable polygon for $j = l, l+1, \ldots$. Similar results are deduced for singular lines ℓ'_j, $j = l, l+1, \ldots$. Hence, the finite set of singular lines $\ell_j \in L, \ell'_j \in L'$, $j = 1, 2, \ldots, l-1$ are sufficient to be used to compute the stable regions in the $k_D - k_I$ plane for each τ.

A similar concept of periodicity frequency is also used in Hermite–Biehler technique of Ou et al. (2009). The roots of the real and the imaginary parts of the characteristic equation interlace for the frequencies larger than this frequency. Hence, just the frequencies smaller than the periodicity frequency are required to be computed.

Remark 4: The real root boundary in $k_I - k_D$ plane is the line $k_I = 0$ and its more stable side is described by

$$k_I > 0, \text{ if } k_p > -b_1/a_0, \; a_0 \neq 0, \tag{57}$$

$$k_I < 0, \text{ if } k_p < -b_1/a_0, \; a_0 \neq 0. \tag{58}$$

The proofs of Equations (57) and (58) is straight forward by setting the frequency in Equations (13) and (14) equal to 0 to obtain the real root boundary (RRB) and using Equation (51) to compute the root crossing direction.

Algorithm

(1) Computing the stable delay interval:
  1.1. Choose a small enough $\varepsilon \ll 1$. Sweep $\omega'_{l'} \in [0, \infty)$ to compute ω_l from the polynomial function (46). Select the pairs ω_l and $\omega'_{l'}$ that satisfy Equation (45).
  1.2. Evaluate τ from Equation (40) for each pair ω_l and $\omega'_{l'}$, and compute $\bar{\omega}(\tau)$ from Equation (37).
  1.3. Calculate $z_{\min}(\tau)$, by substituting $\bar{\omega}(\tau)$ into Equation (39), and $z(\tau)$ as the number of singular frequencies in the interval $(0, \bar{\omega}(\tau))$. Then, compare the diagrams $z(\tau)$ and $z_{\min}(\tau)$ and find the delay interval for which $z(\tau)$ is greater than $z_{\min}(\tau)$. This is the stable delay interval, inside which Equation (38) is satisfied.

(2) Plotting the stable regions in the $k_D - k_I - \tau$ space:
Iterate on τ to sweep the interval computed in Step 1, and do the following in each iteration:

  2.1. Find the value of l so that Equation (36) holds. Then, compute the singular frequencies ω_j and ω'_j, $j = 1, 2, \ldots, l-1$ from Equations (24) and (25).
  2.2. Compute the singular lines ℓ_j and ℓ'_j, $j = 1, 2, \ldots, l-1$ by substituting the singular frequencies of Step 4 into Equations (49) and (50). Then, compute e_I corresponding to each singular line from Equation (52). Mark the upper or lower side of a singular line if $e_I = 1$ or $e_I = -1$ hold, respectively.
  2.3. Mark the upper or lower side of the RRB ($k_I = 0$), respectively, if Equation (58) or (57) holds.
  2.4. Define the stable regions as the regions surrounded by the unmarked sides of singular lines and the RRB.

4. Case study

Consider the second-order, unstable, non-minimum phase time-delay plant of a stirred tank reactor (Rao & Chidambaram, 2006) in Equation (26). A PID controller along with a lead/lag controller structure is tuned to stabilise the plant (26) with a fixed delay of 20s. Here, the controller $C(s)$ is a PID controller with $k_p = 1$ (Figure 1). The algorithm of Section 4 is used to compute the stable domain in the $k_D - k_I - \tau$ space.

Step 1.1: A small value of $\varepsilon = 0.2$ is chosen. Then, $\omega'_{l'}$ in Equation (46) is swept in $\in [0, \infty)$ to compute ω_l. The

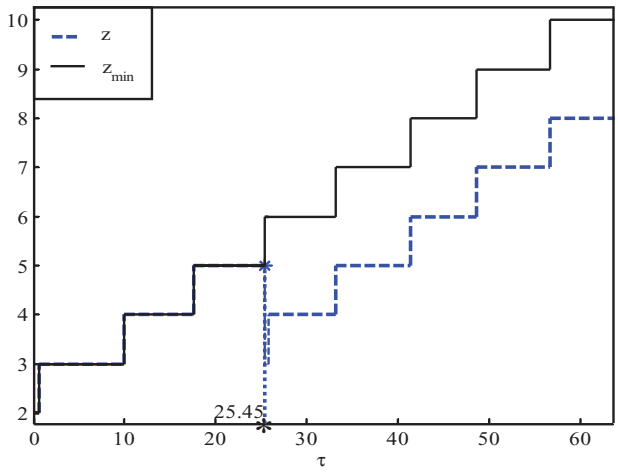

Figure 6. $z_{\min}(\tau)$ and $z(\tau)$.

$\omega_l, \omega'_{l'}$ pairs are chosen to satisfy Equation (45). For instance, $\omega_l = 0.493$ is computed for $\omega'_{l'} = 0.376$.

Step 1.2: For each computed pair, τ is evaluated from Equation (40). For instance, $\tau = 25$ corresponds to $(\omega'_{l'}, \omega_l) = (0.376, 0.493)$. $\bar{\omega}$ corresponding to each τ, equals to $\max\{\omega_l, \omega'_{l'}\}$ from Equation (37). In this case, $\bar{\omega}\ (25) = \max\{0.376, 0.493\} = 0.493$. Figure 2 shows the $\bar{\omega}(\tau)$ diagram. Note that $\bar{\omega}$ is on the horizontal axis. The number of frequencies at the left-hand side of this curve is $z_{\min}(\tau)$. As stated in Remark 1, the sequence $\omega'_2, \omega_5, \omega'_3, \omega_6, \omega'_4, \ldots$ have the periodicity π/τ with precision $\varepsilon = 0.2$ for $\tau = 25$. These frequencies are at the left-hand side of $\bar{\omega}$ (Equation (25)).

Step 1.3: The values $q = 2$, $m_R = 1$ and $m_I = m_o = \hat{m}_I = 0$ are computed using Equation (26). By substituting these values and $\bar{\omega}(\tau)$ in Equation (38), $z_{\min}(\tau) = \text{ceil}[3/2 + \tau\bar{\omega}(\tau)/\pi] - 1$ is computed. For instance, $z_{\min}(25) = \text{ceil}[3/2 + 0.493 * 25/\pi] - 1 = 5$ holds. Also, $z(25) = 5$ is obvious from Figure 2. $z_{\min}(\tau)$ and $z(\tau)$ are plotted in Figure 6. Obviously, $z(\tau)$ exceeds $z_{\min}(\tau)$ in the interval $\tau \in [0, 25.45]$, satisfying Equation (38). Hence, $\tau = 25.45$ is the maximum delay for which stable PID controller exists for $k_p = 1$. It can easily be checked that this maximum can be increased to $\tau = 33.35$ by decreasing k_p to 0.4. The computed interval is swept to perform Step 2. Consider $\tau = 25 \in [0, 25.45]$. The periodicity of the high singular frequencies of Equation (26) for $\tau = 25s$ is already investigated in Remark 1.

Step 2.1: From Remark 1, the singular frequencies $\{\omega_5, \omega_6 \ldots\} \in \Omega$ and $\{\omega'_2, \omega'_3, \ldots\} \in \Omega'$ in Equation (27) tend to the periodicity π/τ with precision $\varepsilon = 0.2$. Hence, from Equation (27), the singular frequencies greater than 0.374 in the Ω set and greater than 0.2598 in the Ω' set, interlace. Hence, the singular frequencies {0.0207, 0.0898, 0.1033, 0.374} in the Ω set, and {0.2598} in the Ω' set, are sufficient to be checked to compute the stable regions.

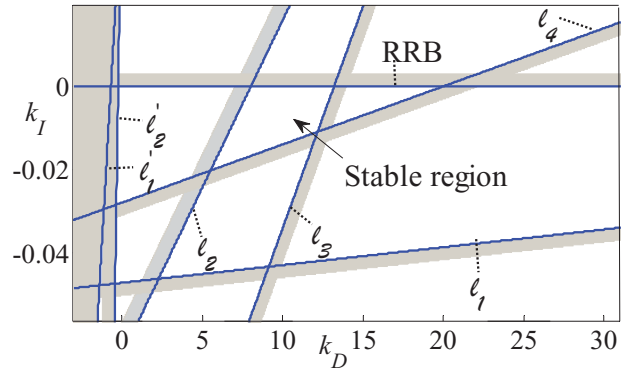

Figure 7. Stable region in $k_D - k_I$ plane for $\tau = 25s$.

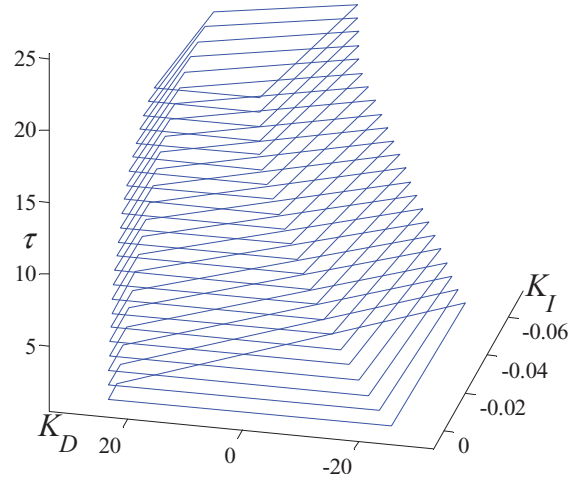

Figure 8. Stable region in the $k_D - k_I - \tau$ space.

Step 2.2: The corresponding singular lines $\ell_1, \ldots, \ell_4$ and ℓ'_1 are computed in the plane of $k_D - k_I$, by substituting the singular frequencies $\{\omega_1, \ldots, \omega_4\} \in \Omega$ and $\{\omega'_1\} \in \Omega'$, respectively, into Equations (49) and (50) (Figure 7). For instance, the SF ℓ_1 is computed as $\ell_1 : k_I - 0.0004k_D + 0.0473 = 0$ by substituting $\omega_1 = 0.0207$ in Equation (49). Also, the more stable side is evaluated from Equation (52). For instance, $e = -1$ is computed by substituting $\omega_1 = 0.0207$ in Equation (52).

Step 2.3: The RRB is the line $k_I = 0$, and its marked side is computed by checking Equations (57) and (58).

Step 2.4: The stable region surrounded by the unmarked sides is shown in Figure 7. By sweeping τ in the stable interval [0, 25.45], the stable region is obtained in the 3D space of $k_D - k_I - \tau$ (Figure 8).

5. Conclusion

Several existing tools are used in this paper to compute an unsolved problem for PID control of time-delay systems with perturbed delays. A general class of time-delay

systems with arbitrary orders is considered. The characteristic equations of the system are transformed to a new space using, the Rekasius substitution. The SF method is reframed here for the RTS. It is shown that, in this case, two generator functions are obtained for computing two sets of singular frequencies. Also, it is proved that the frequencies of two sets interlace with a periodicity of π/τ at high frequencies. Then, two sets of singular line and their features are extracted from the RTS equations. The singular frequencies and periodicity frequency are computed as functions of the uncertain delay. Then, the delay intervals for which stable PID controllers exist, are computed. An algorithm is presented to determine the maximum allowable time delay, for which a stabilising PID controller can be found. To the best of authors' knowledge, no analytic method is available in the literature, to compute this delay. All the previous works have assigned certain values to the time delays to compute the set of all stabilising controllers. Even when uncertain delay is assumed as in Emami and Watkins (2009), a mean value in the range of the uncertainty delay is assumed. This leads to rough estimation of stabilising controllers. Finally, the stability regions in the space of delay and controller coefficients are computed by sweeping the delay in the computed stable range. The extension of the results to compute the range of delay and the controller coefficients to satisfy performance specifications such as reference input tracking and disturbance rejection, is an open area for further research.

Disclosure statement

No potential conflict of interest was reported by the authors.

References

Almodaresi, E., & Bozorg, M. (2009). Stability crossing surfaces for linear time-delay systems with three delays. *International Journal of Control, 82*(12), 2304–2310.

Almodaresi, E., & Bozorg, M. (2014). Computing stability domains in the space of time delay and controller coefficients for FOPDT and SOPDT systems. *Journal of Process Control*, 24(12), 55–61.

Almodaresi, E., & Bozorg, M. (2015). kp stable regions in the space of time delay and PI controller coefficients. *International Journal of Control*, 88(3), 653–662.

Bajcinca, N. (2001). *The method of singular frequencies for robust design in an affine parameter space*. Paper presented at 9th Mediterranean Conference on Control and Automation, Croatia.

Bajcinca, N. (2006). Design of robust PID controllers using decoupling at singular frequencies. *Automatica, 42*(11), 1943–1949.

Chen, J., Gu, G., & Nett, C.N. (1994). *A new method for computing delay margins for stability of linear delay systems*. Paper presented at Proceedings of the 33rd IEEE Conference on Decision and Control, Florida, USA, (Vol. 1, pp. 433–437). IEEE.

Du, B., Lam, J., & Shu, Z. (2010). Stabilization for state/input delay systems via static and integral output feedback. *Automatica, 46*(12), 2000–2007.

Emami, T., & Watkins, J.M. (2009). *Robust stability design of PID controllers for arbitrary-order transfer functions with uncertain time delay*. Paper presented at 41st Southeastern Symposium on System Theory (SSST), Tullahoma, Tennessee (pp. 184–189). IEEE.

Gu, K., Kharitonov, V.L., & Chen, J. (2003). *Stability of time-delay systems*. Boston, MA: Birkhäuser.

Gu, K., Niculescu, S.-I., & Chen, J. (2005). On stability crossing curves for general systems with two delays. *Journal of Mathematical Analysis and Applications, 311*(1), 231–253.

Hohenbichler, N. (2009). All stabilizing PID controllers for time delay systems. *Automatica, 45*(11), 2678–2684.

Hohenbichler, N., & Ackermann, J. (2003). *Computing stable regions in parameter spaces for a class of quasipolynomials*. Paper presented at the IFAC workshop on time delay systems, Rocquencourt, France (Vol. 2003, pp. 43).

Lee, S.C., Wang, Q.-G., & Xiang, C. (2010). Stabilization of all-pole unstable delay processes by simple controllers. *Journal of Process Control, 20*(2), 235–239.

Michiels, W., & VyhlíDal, T. (2005). An eigenvalue based approach for the stabilization of linear time-delay systems of neutral type. *Automatica, 41*(6), 991–998.

Michiels, W., Vyhlídal, T., & Zítek, P. (2010). Control design for time-delay systems based on quasi-direct pole placement. *Journal of Process Control, 20*(3), 337–343.

Nguyen, N., Ishihara, A., Krishnakumar, K., & Bakhtiari-Nejad, M. (2009). *Bounded linear stability analysis-a time delay margin estimation approach for adaptive control*. Paper presented at AIAA Guidance, Navigation, and Control Conference (Vol. 5968), Illinois, USA.

Ou, L.-l., Zhang, W.-d., & Yu, L. (2009). Low-order stabilization of LTI systems with time delay. *IEEE Transactions on Automatic Control, 54*(4), 774–787.

Rao, A.S., & Chidambaram, M. (2006). Enhanced two-degrees-of-freedom control strategy for second-order unstable processes with time delay. *Industrial & Engineering Chemistry Research, 45*(10), 3604–3614.

Rekasius, Z. (1980). A stability test for systems with delays. Paper presented at Proceedings of Joint Automatic Control Conference, Paper No. TP9-A, American Institute of Chemical Engineers.

Saadaoui, K., Elmadssia, S., & Benrejeb, M. (2008). *Stabilizing first-order controllers for n-th order all pole plants with time delay*. Paper presented at 16th Mediterranean Conference on Control and Automation, Corsica, France (pp. 812–817). IEEE.

Sipahi, R., & Olgac, N. (2005). Complete stability robustness of third-order LTI multiple time-delay systems. *Automatica, 41*(8), 1413–1422.

Xiang, C., Wang, Q., Lu, X., Nguyen, L., & Lee, T. (2007). Stabilization of second-order unstable delay processes by simple controllers. *Journal of Process Control, 17*(8), 675–682.

Yi, S., Nelson, P., & Ulsoy, A. (2007). Survey on analysis of time delayed systems via the Lambert W function. *Differential Equations, 14*, 296–301.

Yi, S., Nelson, P.W., & Ulsoy, A.G. (2013). Proportional-integral control of first-order time-delay systems via eigenvalue assignment. *IEEE Transactions on Control Systems Technology, 21*(5), 1586–1594.